

Metal-organic framework materials as nano photocatalyst

A. Majedi¹; F. Davar^{*,2}; A. R. Abbasi¹

¹School of Chemistry, College of Science, University of Tehran, Tehran, Islamic Republic of Iran

²Department of Chemistry, Isfahan University of Technology, Isfahan, 84156-83111, Islamic Republic of Iran

Received 18 April 2015; revised 25 July 2015; accepted 12 August 2015; available online 16 December 2015

ABSTRACT: Photocatalytic degradation of toxic organic compounds in water, soil and air by semiconductor catalysts such as TiO₂ and ZnO has received much attention over the last two decades. However, the low quantum yield, easy agglomeration and difficult post-separation of these inorganic catalysts limit their application for large-scale applications. Metal-organic frameworks (MOFs) are the latest class of ordered porous solids that being intensively studied as a novel class of hybrid inorganic-organic material with ultrahigh porosity, enormous internal surface areas, together with the extraordinary tailorability of structure, dimension, size and shape. Recently exploring performance of MOF as a new nanophotocatalyst is attracting interest of researchers working in the fields of chemistry, chemical engineering, material science and others. Although the photocatalytic application of MOF materials is still at the early stage compared with the other applications of them such as gas storage, separation, biomedical application and heterogeneous catalysis, the currently available results have revealed that the design and construction of MOFs for photocatalyst functionality are very active. The present review aims to introduce MOF materials, the synthesized methods and highlights the progress attempts for using them as a nanophotocatalyst for degradation of pollutants.

Keywords: Environment; Metal organic framework; Nano photocatalyst; Nanoporous materials; Organic dyes degradation.

INTRODUCTION

With the rapid development of global industry, environmental pollution has become a serious problem for mankind [1]. Combustion byproducts, industrial chemicals, surfactants and pesticides have resulted in their undesirable accumulation in the environment. Several pollutants are soluble in water and have been found in groundwater, surface water, drinking water and sewage water. Non-biodegradable character and different nature of these compounds make conventional environmental purification methods (biological, physical and chemical methods) unable to effectively eliminate them [2]. Photocatalysis is one of the advanced oxidation processes (AOPs) that has attracted considerable attention to researchers due to the fact that they can effectively remove environmental pollution under UV and/or visible light. This process is based on the hydroxyl radical production using a photocatalyst. Hydroxyl radicals are a very powerful oxidant capable of oxidizing

a wide range of organic compounds with one or many double bonds [3]. The photocatalytic activity is due to photo-induced electrons and corresponding positive holes that are formed. A good photocatalyst must have high photon conversion efficiency in addition to the high specific surface area [4]. Researchers examine different organic pollutants for exploring the performance of a photocatalyst. Some organic pollutants treated are methyl orange (MO) [5], rhodamine-B (RhB), malachite green (MG) [6], methylene blue (MB) [7], methyl violet (MV) [8], orange G (OG) [9] and phenol compounds [10]. Photocatalytic reactions may occur homogeneously or heterogeneously. In the homogeneous photocatalysis, the photocatalyst and the reactants exist in the same phase. (H₂O₂/UV), photo-fenton, ozone (O₃/UV) and transition metal complexes with photoredox ability are the most usual homogeneous photocatalysts [11]. However, homogeneous photocatalysis has limited industrial applications due to the difficult and costly catalyst separation and recovery as well as the corrosion of the equipment used [12]. In the heterogeneous

✉ *Corresponding Author: Fatemeh Davar
Email: f.davar@gmail.com
Tel.: (+98) 21 3133913289
Fax: (+98) 3133913289

photocatalysis, the reactants are in a different phase from the photocatalyst. This process uses semiconductor particles as photocatalysts [13]. The heterogeneous photocatalysis has main advantages of: complete mineralization or formation of more readily biodegradable intermediates, no need of auxiliary chemicals, no residual formation, easy operation and maintenance for the equipment. Nevertheless, this kind of photocatalysis also has some drawbacks: First of all, low photocatalytic efficiency of the known semiconductors brought by electron-hole recombination and narrow photoresponse, Secondly, the suspended photocatalyst particles contaminate the yield and need to be removed and finally using of small particles that have large surface area to volume ratio and therefore, high surface energy lead to catalyst agglomeration [14]. Therefore, there is an increase in demand for new strategies and photocatalysts to improve photocatalytic efficiency, avoid the filtering process and increase catalyst durability. The best known strategy is immobilizing semiconductor powders onto a suitable supporting matrix [15, 16]. However, the photocatalytic activity of immobilized particles has been often lower due to lower surface area to volume ratio and mass transfer limitations [17]. Nanoporous materials are the best candidate for immobilization of semiconductor photocatalysts because of their high porous nature that gives them a favorable surface area. Nanoporous materials can be subdivided into 3 categories according to the size of the pores: Microporous materials (0.2-2 nm), Mesoporous materials (2-50 nm) and Macroporous materials (50-1000 nm) [18]. They encompass a very broad range, from natural to synthetic, inorganic to organic, and crystalline to amorphous [19]: Nanoporous carbon materials [20], nano/mesoporous silica [21] and zeolites [22] are examples of such materials studied for many years. The photocatalyst containing nanoporous solids show better photocatalysis properties because of: i) They provide a high surface area that has capacity to adsorb organic contaminants from surroundings with subsequent photocatalytic degradation of the adsorbents, ii) by dispersion of photocatalysts in the space pores of a nanoporous solid, transition metals can behave as chromophores and thus help in visible light absorption and iii) nanoporous structures could act as electron donors and as acceptors to the guest species depending on the adsorption site and change the kinetics of electron-hole recombination and influence

the photocatalysis efficiency [23]. Metal organic frameworks (MOFs) are new nanoporous materials that recently take into consideration as novel nanophotocatalyst materials. MOFs are organic-inorganic hybrid structures made up of extended 3D networks of small discrete clusters or metal ions connected through multidentate organic ligands [24, 25]. The crystal framework of MOFs is analogous to that of zeolites and other related purely inorganic porous materials, but there are clear differences between them concerning porosity, range of stability, and feasibility of building a crystal structure by design. In particular, MOFs exhibit values of specific surface areas of up to $3000 \text{ m}^2 \text{ g}^{-1}$ and specific pore volumes of up to 1 g cm^{-3} , which are among the highest values ever reported for any material. MOFs have an extremely wide-open structure in which the free space available for host molecules can reach up to 90% of the crystal volume [26]. Also, in the case of MOFs, it is possible to achieve a fine control over the chemical environment and the topology of the internal voids by selecting appropriate building blocks and the way in which they are connected. However, due to the presence of organic building blocks, MOFs are obviously much less stable than zeolites in thermal and chemical environment. On the other hand, MOFs may show their superior behavior when used in room temperature applications that require a response from the material. As compared to activated carbon and traditional inorganic porous solids, the number of possibilities for combining organic and inorganic moieties to yield a porous material is staggering. The crystalline nature of MOFs permits their structures to be clearly characterized by single-crystal X-ray diffraction. To some extent, MOFs have a higher degree of adjustability and design ability in their structures, when compared to other porous materials Table 1 Compare photocatalysis process on the two reported MOFs and other nanoporous materials in the degradation of methyl orange (MO) as a pollutant model. As revealed from Table 1 the photocatalytic activity of porous material apart from MOFs is active by UV light irradiation or has little efficiency in the visible light. Solar irradiation has about 3-5% UV light. Therefore, the development of photocatalysts for the pollution degradation that respond to visible light and, thus, can effectively utilize sun light, is extremely important. In the above pointed that MOFs have the ability to synthesize with different ligands.

Table 1: Comparison of the photocatalysis process of some nanoporous materials in the degradation of MO.

Nanoporous name	Comment	Ref
Zeolite-Y	10% w/w loading of TiO ₂ on zeolite, MO concentration 5 ppm, visible light source (tungsten 400 W lamp), time 240 min, degradation efficiency 42%.	[104]
Nanoporous silica	TiO ₂ immobilized on silica prepared by 10.04 g fumed silica and 10 mL of butyl titanate precursors, MO concentration 10 ppm, UV light source (15 W), time 24 h, degradation efficiency 100%.	[105]
MCM-41	10% w/w loading of TiO ₂ on MCM-41, MO concentration 2 ppm, UV light source (15 W), time 15 min, degradation efficiency 100%.	[106]
Activated carbon	47% w/w loading of TiO ₂ on activated carbon, MO concentration 1mmol/L, UV light source (40 W), time 160 min, degradation efficiency 100%.	[107]
Zirconium–UiO-66 MOF	Visible light source, MO concentration 10 ppm, time 90 min, degradation efficiency 100%.	[108]
(UTSA-38) MOF	UV-Visible light source, MO concentration 20 ppm, time 120 min, degradation efficiency 100%.	[109]

Putting an auxochromic and bathochromic group in the aromatic ring would shift the absorption wavelength of the parent ligand into the visible-light range give them good photocatalytic property in the visible region.

Historical aspects of MOF

During the development of MOFs, because of the lack of a generally accepted definition, several other parallel appellations were also appeared and used. Despite some varying opinions, it is generally accepted that the work of Hoskins and Robson in 1990, where they introduced a “design” flavor to the construction of 3D MOFs using organic molecular building blocks (ligands) and metal ions, symbolizes a new chapter in studying MOFs [27]. After about 10 years, two milestone MOFs, MOF-5 (Zn₄O(bdc)₃, bdc = 1,4-benzenedicarboxylate) [28] and HKUST-1 (Cu₃(btc)₂, btc = 1,3,5-benzenetricarboxylate) [29], further promoted the development within this field, mainly due to their robust porosity. Shortly thereafter, another representative MOF, MIL-101 (Cr₃O(bdc)₃) [30] with high stability, emerged. Among various names used for these materials, porous coordination polymer (PCP) [31, 32] has been the most widespread, followed by porous coordination network (PCN) [33]. Others include MCP (micro porous coordination polymer) [34], MAF (metal azolate frameworks) [35], ZMOF (zeolite-like metal organic framework) [36] and ZIF (zeoliticimidazolate framework) [37]. On the other hand, following the tradition of zeolite science, some researchers have also used an acronym of the laboratory in which the material prepared was the basis for naming

their materials, as for example in the ITQMOF (Instituto de Tecnología Química metal organic framework) [38], series of MILs (matériaux de l’Institut Lavoisier) [39], HKUST (Hong-Kong University of Science and Technology) [40], SNU (Seoul National University) [41], JUC (Jilin University China) [42], CUK (Cambridge University_KRICT) [43], POST (Pohang University of Science and Technology) [44], and so on. Certainly, using the empirical formula of the material expressing metal, ligands, and their stoichiometry is always popular and used in almost all published papers. In addition, based on the structure of an MOF’s net, O’Keeffe and co-workers proposed a systematic terminology to classify the known structures. A three-letter symbol, such as “dia”, “cub”, etc., or its extension (“pcu-a”, “cub-d”, etc.) has been used to identify a three-dimensional (3D) MOF network with a given geometrical linkage topology [45]. This approach can, thus, help describe and understand structures and also, provide a blueprint for the design of new materials [46].

Synthesis method

Normally, MOF synthesis takes place in a solvent and at temperatures ranging from room temperature to approximately 250°C [47, 48]. The energy is generally introduced using conventional electric heating, i.e., heat is transferred from a hot source, the oven, through convection. Alternatively, energy can also be introduced through other heat creators, such as an electric potential, electromagnetic radiation, ultrasound, or mechanically. The energy source is closely related to the duration, pressure, and energy

per molecule introduced into a system [49]. Each of these parameters can have a strong influence over the product formed and its morphology. In the following, different synthesis routes are described wherein energy is introduced through: Conventional synthesis and by other heat source: Electrochemical Synthesis (an electric potential), Mechanochemical Synthesis (mechanical means), Microwave-Assisted Synthesis (microwave irradiation) and Sonochemical Synthesis (ultrasound).

Conventional synthesis

The reaction temperature is one of the main parameters in the synthesis of MOFs. The term conventional synthesis is usually applied to reactions carried out by conventional electric heating. Conventional synthesis can be divided in two groups, solvothermal and non solvothermal which represent the kind of reaction setups that use. Solvothermal reactions take place in closed vessels (autoclaves) near critical point of the solvent. Nonsolvothermal reactions synthesis requirement is simple and take place below or at the boiling point under ambient pressure. The latter reactions can further be classified as the ones taking place at elevated temperatures or the ones at room-temperature [50, 51]. Methods such as slow diffusion of reactants into each other, solvent evaporation from a solution of reactants, and layering of solutions lead to concentration gradients that allow the formation of MOFs. Concentration gradients can also be done using temperature as a variable, i.e., by slow cooling of the reaction mixture or applying a temperature gradient. Also some important MOFs have even been obtained at room temperature by just mixing the starting materials [52, 53].

Electrochemical synthesis

The electrochemical synthesis of MOFs was first reported in 2005 by researchers at BASF [54]. Their main objective was the exclusion of anions, such as nitrate, perchlorate, or chloride, during the syntheses, which are of interest in large-scale production processes. Rather than using metal salts, they are continuously introduced through anodic dissolution to the reaction medium, which contains the dissolved linker molecules and a conducting salt. The metal deposition at the cathode is avoided by using protic solvents, but in the process, H_2 is formed. Another option is the use of compounds such as acrylonitrile,

acrylic, or maleic esters that are preferentially reduced. Other advantages of the electrochemical route for industrial processes are the possibility to run a continuous process and obtain a higher solid content compared to normal batch reactions [55].

Mechanochemical synthesis

Mechanical force can induce many physical phenomena (mechanophysics) as well as chemical reactions [56]. Mechanochemistry has a long history in synthetic chemistry [57] and it has recently been in inorganic solid-state chemistry, organic synthesis, and polymer science [58, 59]. Its use for the synthesis of porous MOFs was first reported in 2006 [60] and the results of selected mechano chemical studies were summarized recently [61]. In mechanochemical synthesis, the mechanical breakage of intramolecular bonds followed by a chemical transformation takes place; for example, with the solvent-free grinding of $Cu(OAc)_2 \cdot 3H_2O$ and isonicotinic acid [62]. Treatment of the starting materials for 10 min in a 20 mL steel reactor containing a steel ball led to a highly crystalline and single-phase product of $[Cu(INA)_2]$ with acetic acid and water molecules in the pores [63]. These can be removed by thermal activation to yield the guest-free porous compound. Interestingly, the grinding was only required to initiate the reaction. As proven by XRPD experiments, a sample ground for just 1 min yielded a single-phase product in the course of 6 h.

Microwave-Assisted Synthesis

Microwave-assisted synthesis relies on the interaction of electromagnetic waves with mobile electric charges. These can be polar solvent molecules/ions in a solution or electrons/ions in a solid [64]. In the solid, an electric current is formed and heating is due to the electric resistance of the solid. In solution, polar molecules try to align themselves in an electromagnetic field and in an oscillating field so that the molecules change their orientations permanently. Thus, by applying the appropriate frequency, collision between the molecules will take place, leading to an increase in kinetic energy, i.e., temperature of the system. Due to the direct interaction of the radiation with the solution/reactants, MW-assisted heating presents a very energy efficient method of heating. Thus, high heating rates and homogeneous heating throughout the sample are possible. Attention must be paid to the choice of appropriate solvents and selective

energy input, since starting materials may strongly interact with the MW radiation. Microwave ovens suited for materials syntheses allow one to monitor temperature and pressure during the reaction, thus ensuring a more precise control of reaction conditions. Nevertheless, transfer of the syntheses to MW ovens from different vendors is often critical, since these differ in their specifications. MW assisted MOF syntheses have mainly focused on (1) the acceleration of crystallization and (2) the formation of nanoscale products, but it has also been used (3) to improve product purity and (4) help the selective synthesis of polymorphs [65]. For example Choi et al synthesized MW MOF-5 efficiently within several minutes and its physicochemical and textural properties were very similar to those synthesized by the conventional hydrothermal heating [66].

MOF for photocatalyst use

Photocatalytic process

Since Fujishima & Honda (1972) [74] discovered the phenomenon of ultraviolet (UV) light induced photocatalytic splitting of water on a TiO₂ electrode, considerable attention has been directed towards the investigation of photocatalysis. A photocatalytic reaction is stimulated by photons absorbed by a photocatalyst. Separated electrons and holes are formed in the photocatalyst. These charge carriers can move to the surface of the photocatalyst and generate hydroxyl radicals that react with reactants such as pollutants, organic molecules and water. On the basis of the mechanism for photocatalytic reactions, an efficient photocatalyst must have the following properties: (i) its electronic band gap is comparable to the energy of the incident light, (ii) it can produce separable charges, and (iii) it is good in transporting charge carriers so that the migration of photon-generated charges to the catalyst surface is facilitated. In order for a semiconductor to be photochemically active as a sensitizer for the above reaction, the redox potential of the photogenerated valence band hole must be sufficiently positive to generate OH[•] Radicals, which can subsequently oxidize the organic pollutant. The redox potential of the photogenerated conduction band electron must be sufficiently negative to be able to reduce adsorbed O₂ superoxide [75]. TiO₂, ZnO, WO₃, CdS, ZnS, SrTiO₃, SnO₂, WSe₂, Fe₂O₃, etc. can be used as photocatalyst. Among the semiconductors, TiO₂ nanoparticles have been studied extensively [76]. The

anatase phase of titanium dioxide is the material with the highest photocatalytic detoxification [77]. This semiconductor provides the best compromise between stability and catalytic performance. Binary metal sulphide semiconductors such as CdS, CdSe or PbS are regarded as insufficiently stable for catalysis, at least in aqueous media as they readily undergo photoanodic corrosion [78]. These materials are also known to be toxic. The iron oxides are not suitable semiconductors as they readily undergo photocathodic corrosion [79]. The band gap for ZnO (3.2 eV) is equal to that of anatase. ZnO however, is also unstable in water with Zn(OH)₂ being formed on the particle surface [80]. This results in catalyst deactivation. Also, the quantum yield and solar energy conversion efficiency of these developed photocatalysts, are still low, thus limiting their practical applications in environmental purification. Consequently, it is of great interest to search for new photocatalysts with improved activities [81].

Photocatalytically active sites in metal organic framework

The MOF-based catalysts are mainly classified into three types: MOFs with metal-active sites, MOFs with reactive functional groups and MOFs as host matrices or nanometric reactors [82]. The catalytic activities observed for MOFs with metal-active sites are directly related to the metallic components, either as isolated metal centers or as clusters connected through the organic linkers. Thus, MOFs with metal-active sites can be regarded as single-site catalysts. The first study of a MOF as a photocatalyst to degrade organic pollutants have been reported by Mahata et al in 2006 [83]. They synthesized three metal-organic frameworks (MOFs): [Co₂(C₁₀H₈N₂)] [C₁₂H₈O(COO)₂]₂ (1), [Ni₂(C₁₀H₈N₂)₂] [C₁₂H₈O-(COO)₂]₂·H₂O (2) and [Zn₂(C₁₀H₈N₂)] [C₁₂H₈O(COO)₂]₂ (3), with three-dimensional structures. The structures of the three compounds appear somewhat related, formed by the connectivity involving the metal polyhedra (Co₄N trigonal bipyramids in 1, NiO₄N₂ octahedra in 2, and ZnO₄ tetrahedra and ZnO₃N₂ trigonal bipyramids in 3). The photocatalytic studies on these MOF reveal that they are more active than P25 for the degradation of orange G, rhodamine. B, Remazol Brilliant Blue R, and methylene blue. One of the most common materials, denoted as MOF-5, contains clusters of Zn₄O located at the corners of the structure connected

orthogonally to six units of terephthalate. Tachikawa *et al.* [84] reported studies on the nature of luminescence transitions in MOF-5 nanoparticles, and the interfacial charge transfer from the photoexcited MOF-5 to various organic compounds. It was revealed that MOF-5 had a much higher oxidation reaction efficiency than that of P-25 TiO₂ powder, the most common photocatalyst. Xamena *et al.* Used MOF-5 as photocatalyst for the degradation of phenol and 2, 6-di-*tert*-butylphenol (DTBP) [85] Fig. 1 shows TEM images of MOF-5 nanoparticles before and after water treatment.

Fig. 2 shows photodegradation curve of phenol and

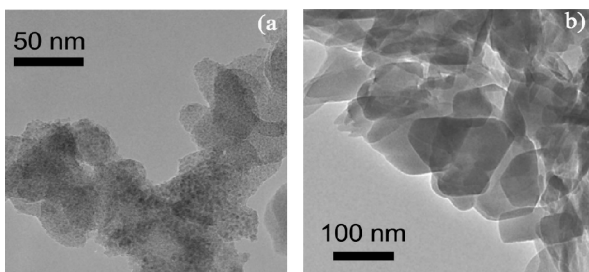


Fig. 1: TEM image of MOF-5 nanoparticles a) before and b) after water treatment [85].

2, 6-di-*tert*-butylphenol. The results obtained for MOF-5 as a photocatalyst indicate that large molecules (i.e., molecules with a high steric hindrance with respect to the pore openings of MOF-5) are degraded faster. The authors explained the different behavior of the material

toward small and large molecules by adducing that small molecules can freely diffuse to the internal space of the material, where they are less prone to undergo photodegradation. In contrast, bulky molecules remain at the external surface of the photocatalyst, where they are rapidly degraded. In other words, degradation of the organic molecules takes place at a different rate in the internal and external surface of the photocatalyst (being significantly lower at the internal surface). Conclusion is that MOF-5 exhibits a reverse shape-selectivity photocatalyst. Solid lines are the best fit to experimental data obtained with a first order exponential decay. Dotted straight lines show the initial degradation rates. Fig. 3 shows the mechanism of phenol degradation upon the MOF-5 [85]. Alvaro *et al.* calculated the band gap of MOF-5 as a semiconductor from the plot of the reflectance versus the radiation energy, giving a value of 3.4 eV [86]. In order to get an estimation of these energy values, they proceeded to construct a photovoltaic cell using MOF-5 as a semiconductor. The position of the conduction band was determined by comparison of the open circuit voltage obtained for a photovoltaic cell constructed with I₂/I⁻ as the electrolyte and TiO₂ or MOF-5 as the photoactive semiconductor. The conduction band position for TiO₂ (0.1 eV) has been reported in the literature [87].

The conduction band energy of MOF-5, 0.2 V versus NHE has been estimated considering that the

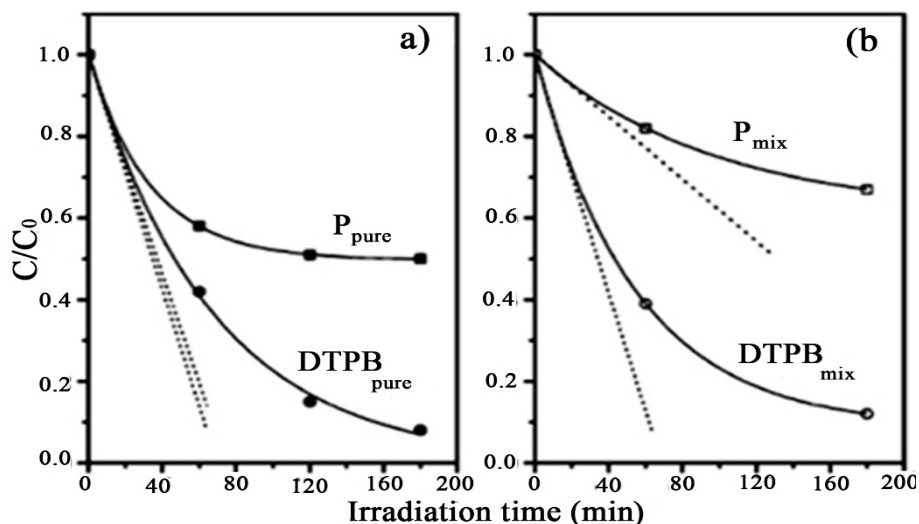


Fig. 2: Photodegradation curves of phenol (P) and 2, 6-di-*tert*-butylphenol (DTBP) obtained using MOF-5 as a photocatalyst. a) Curves correspond to photodegradation of 40 ppm of pure species b) curves correspond to competitive photodegradation (irradiation of a mixture of 20 ppm of both molecules) [63].

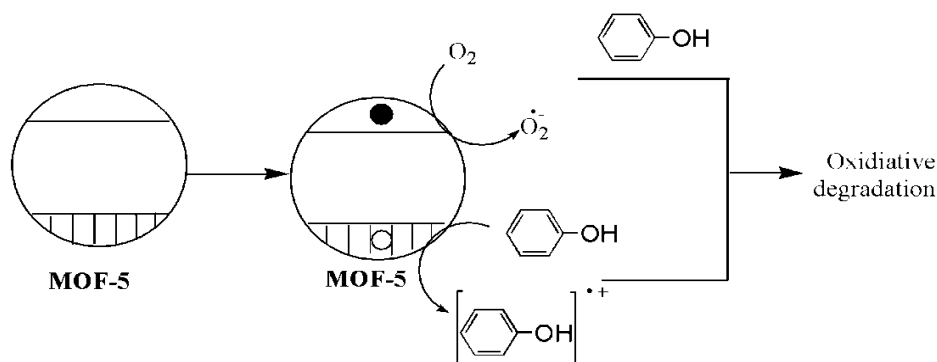


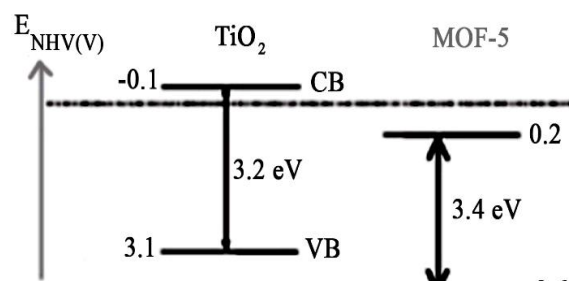
Fig. 3: Propose mechanism of phenol degradation upon the MOF-5[85].

photovoltaic cell with MOF-5 gives a value of open current voltage that is 0.3 V lower than the one obtained for a solar cell with TiO_2 . Then, they proceeded to determine the percentage of phenol degradation upon irradiation through Pyrex in identical aqueous suspensions of phenol containing MOF-5, standard P-25 TiO_2 and ZnO. They selected ZnO for comparison because in case the MOF-5 would undergo structural damage in a small percentage, ZnO could be formed. The results revealed MOF-5 exhibited a remarkable photocatalytic activity. Comparison between the performance of MOF-5 and other as in the case of titanium dioxide showed that photodegradation of phenol might occur through a network of reactions including the initial formation of radical cation by electron transfer from phenol to MOF-5 hole or generation of oxygen active species by the reaction of the photoejected electrons with oxygen. Fig. 4 summarizes a possible mechanistic proposal. It can be easily anticipated that the relative photocatalytic activity of MOF-5 with respect to the other photocatalysts will most probably vary depending on the light source. In particular, visible irradiation using filtered light (cut-off filter $\lambda > 380$ nm) would strongly disfavor the activity of TiO_2 and ZnO due to their lack of absorption at wavelength > 350 nm while MOF-5 is absorbed above 350 nm. Other traditional MOFs are IRMOF1 stands for isoreticular metal-organic framework 1 and $M = \text{Be}, \text{Mg}, \text{Ca}, \text{Zn},$ and Cd . Cabrera et al examined the electronic structure of M -IRMOF1 using density-functional theory [88].

The results showed that these materials had similar band gaps 3.5 eV and a conduction band split into two bands, the lower of which had a width that varied with metal substitution. After doping Zn-IRMOF1 and Be-IRMOF1 with Al or Li, they investigated electronic

properties of the materials. It was shown that replacing one metal atom with Al could effectively be used to create IRMOFs with different metallic properties. On the other hand, adding Li produced structural changes that rendered this approach less suitable. Lanthanide-based metal-organic frameworks (Ln-MOFs), especially Tb^{3+} and Eu^{3+} , are fascinating because of their versatile coordination geometry, unique luminescent and magnetic properties, and possible high framework stability to water [89, 90]. Choi and coworkers reported systematic studies of interfacial electron transfer between photoexcited europium-based MOF (Eu-MOF) particles and various organic compounds, such as aromatic sulfides and amines adsorbed on the surface and trapped inside the pores of the MOF structure (Fig. 5) [74]. The 1,3,5-benzenetribenzoate (BTB) ligand was chosen as a linker and they selected the Eu^{3+} ion as the constituent metal because Eu^{3+} had a very low reduction potential ($E_{\text{red}}(\text{Eu}^{3+}/\text{Eu}^{2+}) = -0.35$ V vs NHE) and the resultant Eu^{2+} ion could be reoxidized to its initial state by various oxidants such as O_2 and H_2O_2 .

Eu^{3+} ions were in the Eu-MOF with the organic compounds. They discovered the size-selective one-

Fig. 4: Band gap energy of TiO_2 vs MOF-5[87].

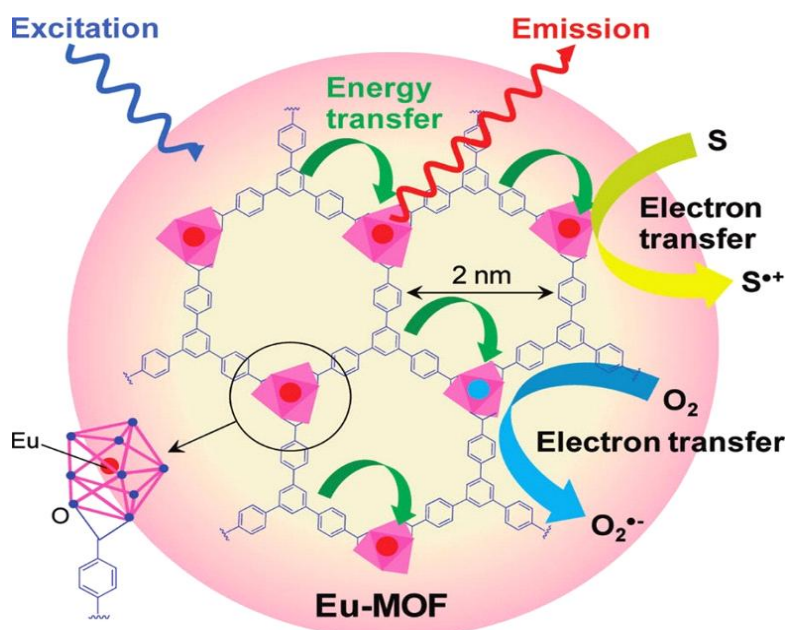


Fig. 5: PhotoexcitedEu-MOF [74].

electron oxidation processes of organic compounds under the photo irradiation of nanosized and microsized Eu-MOF particles by combining time-resolved emission and absorption spectroscopy, confocal microscopy, and a theoretical calculation based on the Marcus theory. They concluded confidently that there was the possibility that Eu-MOFs work as an efficient photocatalyst under UV light irradiation. They predicted that in the future, by varying the length of the organic backbone of the ligands and changing the degree of conjugation in the ligands, molecular recognition MOF photocatalysts extending their photosensitivity toward the visible-light region will be developed.

Yang *et al* synthesized ZnO-based nanostructured architectures via simple heat treatment of MOF-5 under different atmospheric conditions. In air, MOF-5 was transformed into hierarchical aggregates of ZnO nanoparticles with 3D cubic morphologies [91]. The resultant materials showed good photocatalytic activity with respect to RhB degradation such that the degradation rate constants were comparable to that of commercial P25 and much higher than that of ST01. Titanium is a very attractive candidate for MOFs due to its low toxicity, redox activity, and photocatalytic properties. Hardi synthesized MIL-125, the first example of a highly porous and crystalline titanium (IV)

dicarboxylate (MIL stands for Materials of Institute Lavoisier), with a high thermal stability and photochemical properties. Its structure is built up from a pseudo cubic arrangement of octameric wheels built up from edge- or corner-sharing titanium octahedra, and terephthalate dianions, thereby leading to a three-dimensional periodic array of two types of hybrid cages with accessible pore diameters of 6.13 and 12.55 Å [92]. Walsh *et al.* [93] examined the electronic and defect structure of a novel hybrid titania material and confirmed the spatial separation of electrons and holes between the inorganic and organic sub-networks. Chemical reduction of Ti (IV) to Ti (III) can be readily achieved through intrinsic defect formation (oxygen loss) or extrinsic reductants (e.g. H₂). The remarkably low energy for these processes, which is less than those in bulk TiO₂ and below the band gap energy, explains the facile color change of this material after irradiation under UV light: photostimulated chemical reduction. Gascon *et al.* have showed that by applying operando IR spectroscopy, MOFs are a potentially new class of photocatalysts for selective gas-phase photooxidation [94]. Isorecticular MOFs with different organic linkers were synthesized; namely, terephthalic acid (IRMOF-1), 2-bromoterephthalic (IRMOF-2) acid, 2,5-dibromoterephthalic acid, biphenyl-4,4'-dicarboxylic acid (IRMOF-9), 1,4 naphthalene-dicarboxylic (IRMOF-

7) acid and 2,6-naphthalenedicarboxylic (IRMOF-8) acid using two different solvents (N,N-dimethylformamide (DMF) and N,N-diethylformamide (DEF). They demonstrated that the band gap energy of isorecticular metal-organic frameworks could be tuned by changing the organic linker. Du *et al.* have shown a novel series of photocatalysts based on MIL-53(M) (M= Fe, Cr, Al) metal-organic frameworks for MB photodegradation [95]. The photodegradation of MB over MIL-53(Fe) photocatalyst followed first-order kinetics, and the rate constant was 0.0133 min^{-1} and 0.0036 min^{-1} for UV-Vis light and visible light irradiation, respectively. Furthermore, they presented the large promoting effect of electron acceptor H_2O_2 , KBrO_3 and $(\text{NH}_4)_2\text{S}_2\text{O}_8$ addition on the photocatalytic performance of MIL-53(Fe) photocatalyst. The metal centers of MIL-53 showed a nil effect on the photocatalytic activity for MB photodegradation. Fig. 6 shows the chemical structure and electron transfer upon the MIL-53(Fe). Zhang *et al.* investigated the iron-based MIL-53(Fe) metal-organic framework in the degradation of RhB.

Fig. 7 shows comparison of the reaction rate constants of the degradation of RhB in different

conditions. The catalytic degradation of RhB proceeded about 4.3 and 4.6 times faster in the MIL-53(Fe)/visible light/ H_2O_2 system, relative to the MIL-53/visible light system and MIL-53(Fe)/ H_2O_2 system, respectively [96]. Attempts to obtain robust MOFs with high photocatalytic activity have met with only limited success. One important reason is due to that the most MOFs are not able to absorb visible light or lack catalytic sites for the photocatalysis process. The tunable nature of the organic components in MOFs allows them to readily functionalize. According to literatures, two common strategies have been employed in the post synthesis modification to activate MOFs.[97, 98]. One of the approaches is doping MOFs with light-absorbing metalcomplexes [99]. Another approach is introduction of the light absorbing organic building units. this method porphyrins [100] and 2-aminoterephthalate [101-103] ligandes, are two example that use as linkers in the MOFs synthesis in order to harvest visible light. Table 2 shows some recent used MOFs and for the degradation of organic pollutants.

CONCLUSION

The field of heterogeneous photocatalysis is very

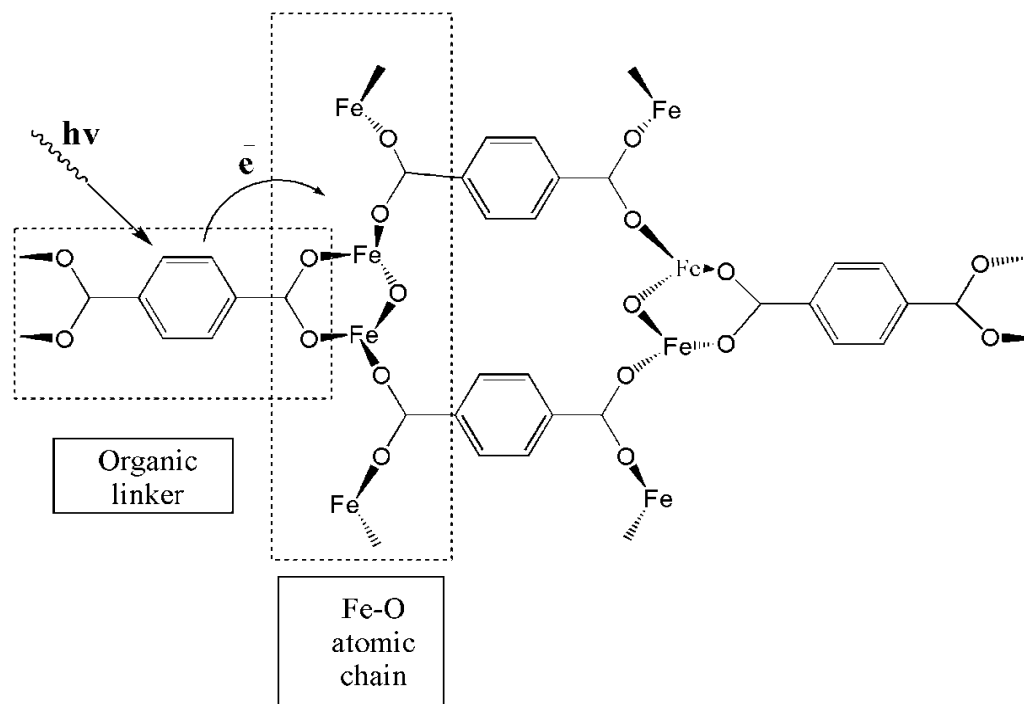


Fig. 6: The chemical structure of MIL-53(Fe) and electron transfer processes that occur in MIL-53(Fe) when irradiated by light [95].

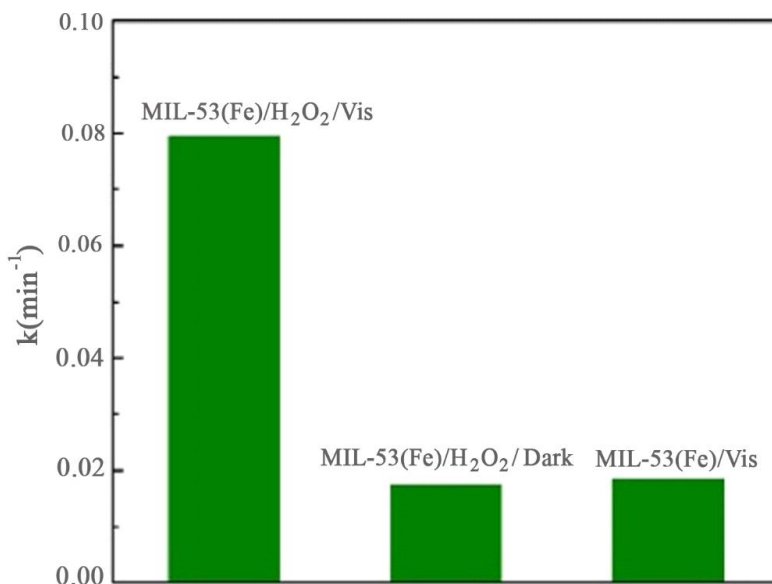


Fig. 7: Comparison of the apparent reaction rate constants of the degradation of RhB under different conditions [96].

Table 2: Some compounds degraded by various researchers using different MOFs.

Degraded Compound	MOF used	Light source	Degradation efficiency (%)	Time (min)	Ref
rhodamine-B (RhB)	{Na ₄ (H ₂ O) ₁₂ [Fe ^{II}] ₂ [Fe ^{III}] ₄ (PO ₄) ₆][Fe ^{III} (Mo ₆ O ₁₉) ₂ (PO ₄) ₈] ₂ }(OH) ₃ ·33H ₂ O	300 W Xe lamp	100	240	[110]
malachite green (MG)	MIL-53(Fe)	300 W Xe lamp	60	300	[111]
rhodamine-B (RhB)	MIL-53(Fe)	300 W Xe lamp	80	300	[111]
orange G (OG)	[Cu(O ₂ NCP)(4,4'-H ₂ BPA)1/2(H ₂ O)(4,4'-H ₂ BPA)] _n	500 W tungsten lamp	38.61	300	[112]
rhodamine B (RhB)	[Cu(O ₂ NCP)(4,4'-H ₂ BPA)1/2(H ₂ O)(4,4'-H ₂ BPA)] _n	500 W tungsten lamp	12.68	300	[112]
methylene blue (MB)	[Cu(O ₂ NCP)(4,4'-H ₂ BPA)1/2(H ₂ O)(4,4'-H ₂ BPA)] _n	500 W tungsten lamp	71.61	300	[112]
methyl violet (MV)	[Cu(O ₂ NCP)(4,4'-H ₂ BPA)1/2(H ₂ O)(4,4'-H ₂ BPA)] _n	500 W tungsten lamp	25.39	300	[112]
orange G (OG)	[Zn(TBTC)(2,6-pydc)] _n	500 W Xe lamp	53	270	[113]
rhodamine B (RhB)	[Zn(TBTC)(2,6-pydc)] _n	500 W Xe lamp	80	270	[113]
methylene blue (MB)	[Zn(TBTC)(2,6-pydc)] _n	500 W Xe lamp	79	270	[113]
methyl violet (MV)	[Zn(TBTC)(2,6-pydc)] _n	500 W Xe lamp	90	270	[113]
orange G (OG)	[Co ₂ (1,4-BDC)(NCP)2]n·4nH ₂ O	500 W tungsten lamp	67.59	300	[114]
rhodamine B (RhB)	[Co ₂ (1,4-BDC)(NCP)2]n·4nH ₂ O	500 W tungsten lamp	67.52	300	[114]
methylene blue (MB)	[Co ₂ (1,4-BDC)(NCP)2]n·4nH ₂ O	500 W tungsten lamp	62.75	300	[114]
methyl violet (MV)	[Co ₂ (1,4-BDC)(NCP)2]n·4nH ₂ O	500 W tungsten lamp	33.29	300	[114]

diverse. The traditional photocatalysts have some drawbacks such as low quantum yield and UV source as the induction of reaction. Because of these reasons, research on new photocatalysts is an interesting field in science. In this paper, novel nano photocatalysts based on MOF materials have been introduced and recent works in these filed have been reviewed.

REFERENCES

- [1] Ribeiro A.R., Nunes O.C., Pereira M. F. R., Silva A. M. T., (2015), An overview on the advanced oxidation processes applied for the treatment of water pollutants defined in the recently launched Directive 2013/39/EU. *Environ. Inter.* 75: 33-51.
- [2] Ibhaddon A., Fitzpatrick P., (2013), Heterogeneous Photocatalysis: Recent Advances and Applications. *Catalysts*. 3: 189-218.
- [3] Spasiano D., Marotta R., Malato S., Fernandez-Ibañez P., Di Somma L., (2015), Solar photocatalysis: Materials, reactors, some commercial, and pre-industrialized applications. A comprehensive approach. *Appl. Cat. B: Environ.* 170–171: 90-123.
- [4] Kočí K., Obalová L., Matějová L., Plachá D., Lacný Z., Jirkovský J., Šolcová O., (2009), Effect of TiO₂ particle size on the photocatalytic reduction of CO₂. *Appl. Catal. B.: Environ.* 89: 494-502.
- [5] Kaur J., Bansal S., Singhal S., (2013), Photocatalytic degradation of methyl orange using ZnO nanopowders synthesized via thermal decomposition of oxalate precursor method. *Physica B: Condens. Matter.* 416: 33-38.

- [6] You-ji L., Wei C., (2011), Photocatalytic degradation of Rhodamine B using nanocrystalline TiO₂-zeolite surface composite catalysts: effects of photocatalytic condition on degradation efficiency. *Catal. Sci. & Tech.* 1: 802-809.
- [7] Tayade R. J., Natarajan T. S., Bajaj H. C., (2009), Photocatalytic Degradation of Methylene Blue Dye Using Ultraviolet Light Emitting Diodes. *Indus. & Eng. Chem. Res.* 48: 10262-10267.
- [8] Gupta A. K., Pal A., Sahoo C., (2006), Photocatalytic degradation of a mixture of Crystal Violet (Basic Violet 3) and Methyl Red dye in aqueous suspensions using Ag⁺ doped TiO₂. *Dyes and Pigm.* 69: 224-232.
- [9] Sun J., Wang X., Sun J., Sun R., Sun S., Qiao L., (2006), Photocatalytic degradation and kinetics of Orange G using nano-sized Sn(IV)/TiO₂/AC photocatalyst. *J. Molec. Catal. A: Chemical.* 260: 241-246.
- [10] Ahmed S., Rasul M. G., Martens W. N., Brown R., Hashib M. A., (2010), Heterogeneous photocatalytic degradation of phenols in wastewater: A review on current status and developments. *Desalination.* 261: 3-18.
- [11] Cieřla P., Kocot P., Mytych P., Stasicka Z., (2004), Homogeneous photocatalysis by transition metal complexes in the environment. *J. Molec. Catal. A: Chemical.* 224: 17-33.
- [12] Kim S., Park H., Choi W., (2004), Comparative Study of Homogeneous and Heterogeneous Photocatalytic Redox Reactions: PW12O₄₀3- vs TiO₂. *J. Phys. Chem. B.* 108: 6402-6411.
- [13] Davar F., Majedi A., Mirzaei A., (2015), Green Synthesis of ZnO Nanoparticles and Its Application in the Degradation of Some Dyes. *J. Am. Ceramic Soc.* 1: 1-8.
- [14] Xuan J., Xiao W.-J., (2012), Visible-Light Photoredox Catalysis. *Ang. Chem, Int, Ed.* 51: 6828-6838.
- [15] Phanikrishna Sharma M. V., Sadanandam G., Ratnamala A., Durga Kumari V., Subrahmanyam M., (2009), An efficient and novel porous nanosilica supported TiO₂ photocatalyst for pesticide degradation using solar light. *J. Hazard. Mater.* 171: 626-633.
- [16] Muthirulan P., Meenakshisundararam M., Kannan N., (2013), Beneficial role of ZnO photocatalyst supported with porous activated carbon for the mineralization of alizarin cyanin green dye in aqueous solution. *J. Adv. Res.* 4: 479-484.
- [17] Xu Y., Langford C. H., (1997), Photoactivity of Titanium Dioxide Supported on MCM41, Zeolite X, and Zeolite Y. *J. Phys. Chem. B.* 101: 3115-3121.
- [18] Zdravkov B., Čermák J., Šefara M., Janků J., (2007), Pore classification in the characterization of porous materials: A perspective. *Cen. Europ. J. Chem.* 5: 385-395.
- [19] Sing K. S.W., Schüth F., (2008), Handbook of Porous Solids, 24-33, *Wiley-VCH Verlag GmbH.*
- [20] Geranmayeh S., Abbasi A., Badiei A., (2011), Synthesis and Characterization of Nanoporous Carbon Materials. The Effect of Surfactant Concentrations and Salts. *E-Journal Chem.* 8: 54-59.
- [21] Badiei A., Gholami J., Khaniani Y., (2009), Synthesis and Characterization of Titanium Supported on High Order Nanoporous Silica and Application for Direct Oxidation of Benzene to Phenol. *E-Journal Chem.* 6: 88-91.
- [22] Davis M. E., Lobo R. F., (1992), Zeolite and molecular sieve synthesis. *Chem. Mater.* 4: 756-768.
- [23] Subotić B., Bronić J., Antić Jelić T., (2009), Ordered Porous Solids. Valtchev, V., Mintova, S. and Tsapatsis, M. (eds), 127-185, *Elsevier, Amsterdam.*
- [24] Stock N., Biswas S., (2012), Synthesis of Metal-Organic Frameworks (MOFs): Routes to Various MOF Topologies, Morphologies, and Composites. *Chem. Rev.* 112: 933-969.
- [25] Cohen S. M., (2012), Postsynthetic Methods for the Functionalization of Metal-Organic Frameworks. *Chem. Rev.* 112: 970-1000.
- [26] Rowsell J. L. C., Yaghi O. M., (2004), Metal-organic frameworks: a new class of porous materials. *Microp. and Mesop. Mater.* 73: 3-14.
- [27] Hoskins B. F., Robson R., (1990), Design and construction of a new class of scaffolding-like materials comprising infinite polymeric frameworks of 3D-linked molecular rods. A reappraisal of the zinc cyanide and cadmium cyanide structures and the synthesis and structure of the diamond-related frameworks [N(CH₃)₄][CuI₂ZnII(CN)₄] and CuI[4,4',4'',4'''-tetracyanotetraphenylmethane]BF₄.xH₂O. *J. Am. Chem. Soc.* 112: 1546-1554.
- [28] Li H., Eddaoudi M., O'Keeffe M., Yaghi O. M., (1999), Design and synthesis of an exceptionally stable and highly porous metal-organic framework. *Nature.* 402: 276-279.
- [29] Chui S. S.-Y., Lo S. M.-F., Charmant J. P. H., Orpen A. G., Williams, I.D. (1999), A Chemically Functionalizable Nanoporous Material [Cu₃(TMA)₂(H₂O)₃]n. *Science.* 283: 1148-1150.
- [30] Park H. J., Suh M. P., (2008), Mixed-Ligand Metal-Organic Frameworks with Large Pores: Gas Sorption Properties and Single-Crystal-to-Single-Crystal Transformation on Guest Exchange. *Chem. An Europ. J.* 14: 8812-8821.
- [31] Batten S. R., Champness N. R., Chen X.-M., Garcia-Martinez J., Kitagawa S., Ohrstrom L., O'Keeffe M., Suh M. P., Reedijk J., (2012), Coordination polymers, metal-organic frameworks and the need for terminology guidelines. *Cryst. Eng. Comm.* 14: 3001-3004.
- [32] Abbasi A., Geranmayeh S., Skripkin M. Y., Eriksson L., (2012), Potassium ion-mediated non-covalent bonded coordination polymers. *Dalton Transact.* 41: 850-859.
- [33] Lin J.-B., Zhang J.-P., Chen X.-M., (2010), Nonclassical Active Site for Enhanced Gas Sorption in Porous Coordination Polymer. *J. Am. Chem. Soc.* 132: S 6654-6656.
- [34] Cychosz K. A., Wong-Foy A. G., Matzger A. J., S (2008), Liquid Phase Adsorption by Microporous Coordination Polymers: Removal of Organosulfur Compounds. *J. Am. Chem. Soc.* 130: 6938-6939.
- [35] Fang Q.-R., Makal T. A., Young M. D., Zhou H.-C., (2010), Recent advances in the study of mesoporous metal-organic frameworks Comments. *Inorg. Chem.* 31: 165-195.
- [36] Liu Y., Kravtsov V. C., Larsen R., Eddaoudi M., (2006), Molecular building blocks approach to the assembly of zeolite-like metal-organic frameworks (ZMOFs) with extra-large cavities. *Chem. Comm.* 1488-1490.
- [37] Park K. S., Ni Z., Côté A. P., Choi J. Y., Huang R., Uribe-Romo F. J., Chae H. K., O'Keeffe M., Yaghi O. M., (2006), Exceptional chemical and thermal stability of zeolitic imidazolate frameworks. Proceedings of the National Acad. Sci. 103: 10186-10191.
- [38] Harbuzaru B. V., Corma A., Rey F., Atienzar P., Jordá J. L., García H., Ananias D., Carlos L. D., Rocha J., (2008), Metal-Organic Nanoporous Structures with Anisotropic Photoluminescence and Magnetic Properties and Their Use as Sensors. *Ang. Chem. Int. Ed.* 47: 1080-1083.
- [39] Janiak C., Vieth J. K., (2010), MOFs, MILs and more: concepts, properties and applications for porous

- coordination networks (PCNs). *New J. Chem.* 34: 2366-2388.
- [40] Qiu S., Zhu G., (2009), Molecular engineering for synthesizing novel structures of metal–organic frameworks with multifunctional properties. *Coordin. Chem. Rev.* 253: 2891-2911.
- [41] Humphrey S. M., Chang J.-S., Jhung S. H., Yoon J. W., Wood P. T., (2007), Porous Cobalt(II)–Organic Frameworks with Corrugated Walls: Structurally Robust Gas-Sorption Materials. *Ang. Chem. Int. Ed.* 46: 272-275.
- [42] Seo J. S., Whang D., Lee H., Jun S. I., Oh J., Jeon Y. J., Kim K., (2000), A homochiral metal-organic porous material for enantioselective separation and catalysis. *Nature.* 404: 982-986.
- [43] Yoon J.W., Jhung S. H., Hwang Y. K., Humphrey S. M., Wood P. T., Chang J. S., (2007), Gas-Sorption Selectivity of CUK-1: A Porous Coordination Solid Made of Cobalt(II) and Pyridine-2,4- Dicarboxylic Acid. *Adv. Mater.* 19: 1830-1834.
- [44] An J., Geib S. J., Rosi N. L., (2009), Cation-Triggered Drug Release from a Porous Zinc–Adeninate Metal–Organic Framework. *J. Am. Chem. Soc.* 131: 8376-8377.
- [45] Ockwig N. W., Delgado-Friedrichs O., O’Keeffe M., Yaghi O. M., (2005), Reticular Chemistry: Occurrence and Taxonomy of Nets and Grammar for the Design of Frameworks. *Accoun. Chem. Res.* 38: 176-182.
- [46] Batten S. R., Neville S. M., Turner D. R., (2009), Coordination Polymers: Design, Analysis and Application. 238-256, *The Royal Society of Chemistry.*
- [47] Geranmayeh S., Abbasi A., Skripkin M. Y., Badiei A., (2012), A novel 2D zinc metal–organic framework: Synthesis, structural characterization and vibrational spectroscopic studies. *Polyhedron.* 45: 204-212.
- [48] Abbasi A., Tarighi S., Badiei A., (2012), A three-dimensional highly stable cobalt(II) metal–organic framework based on terephthalic acid: synthesis, crystal structure, thermal and physical properties. *Trans. Metal Chem.* 37: 679-685.
- [49] Geranmayeh S., Abbasi A., (2013), Simultaneous Growing of Two New Cd(II) Metal–Organic Frameworks with 2,6-Naphthalendicarboxylic Acid as New Precursors for Cadmium(II) Oxide Nanoparticles: Thermal, Topology and Structural Studies. *J. Inorg. Organomet. Polymers and Mater.* 23: 1138-1144.
- [50] Abbasi A., Geranmayeh S., Vala S., Juibari N., Badiei A., (2012), Synthesis and characterization of tetrapyridophenazine ligand and its novel 1-D metal-organic wave-like coordination polymer of Ni(II) ion. *Zeitschrift für Kristallographie - Crystall. Mater.* 227: 688-693.
- [51] Bang J. H., Suslick K. S., (2010), Applications of Ultrasound to the Synthesis of Nanostructured Materials. *Adv. Mater.* 22: 1039-1059.
- [52] Geranmayeh S., Abbasi A., Zarnani A.-H., Skripkin M. Y., (2013), A novel trinuclear zinc metal–organic network: Synthesis, X-ray diffraction structures, spectroscopic and biocompatibility studies. *Polyhedron* 61: 6-14.
- [53] Tarighi S., Abbasi A., Geranmayeh S., Badiei A., (2013), Synthesis of a New Interpenetrated Mixed Ligand Ni(II) Metal–Organic Framework: Structural, Thermal and Fluorescence Studies and its Thermal Decomposition to NiO Nanoparticles. *J. Inorg. Org. Polym. Mater.* 23: 808-815.
- [54] Tranchemontagne D. J., Hunt J. R., Yaghi O. M., (2008), Room temperature synthesis of metal-organic frameworks: MOF-5, MOF-74, MOF-177, MOF-199, and IRMOF. *Tetrahedron.* 64: 8553-8557.
- [55] Cravillon J., Münzer S., Lohmeier S.-J., Feldhoff A., Huber K., Wiebcke M., (2009), Rapid Room-Temperature Synthesis and Characterization of Nanocrystals of a Prototypical Zeolitic Imidazolate Framework. *Chem. Mater.* 21: 1410-1412.
- [56] Klimakow M., Klobes P., Thünemann A. F., Rademann K., Emmerling F., (2010), Mechanochemical Synthesis of Metal–Organic Frameworks: A Fast and Facile Approach toward Quantitative Yields and High Specific Surface Areas. *Chem. of Mater.* 22: 5216-5221.
- [57] Ameloot R., Stappers L., Fransaeer J., Alaerts L., Sels B. F., De Vos D. E., (2009), Patterned Growth of Metal-Organic Framework Coatings by Electrochemical Synthesis. *Chem. Mater.* 21: 2580-2582.
- [58] Fernández-Bertran J. F., (1999), Mechanochemistry: An overview. *Pure and Appl. Chem.* 71: 581-586.
- [59] Boldyrev V. V., Tkáčová K., (2000), Mechanochemistry of Solids: Past, Present, and Prospects. *J. Mater. Syn. Proces.* 8: 121-132.
- [60] Beyer M. K., Clausen-Schaumann H., (2005), Mechanochemistry: The Mechanical Activation of Covalent Bonds. *Chem. Rev.* 105: 2921-2948.
- [61] Kaupp G., (2009), Mechanochemistry: the varied applications of mechanical bond-breaking. *Cryst. Eng. Comm.* 11: 388-403.
- [62] Garay A. L., Pichon A., James S. L., (2007), Solvent-free synthesis of metal complexes. *Chem. Soc. Rev.* 36: 846-855.
- [63] Pichon A., Lazuen-Garay A., James S. L., (2006), Solvent-free synthesis of a microporous metal-organic framework. *Cryst. Eng. Comm.* 8: 211-214.
- [64] Friscic T., (2010), New opportunities for materials synthesis using mechanochemistry. *J. Mater. Chem.* 20: 7599-7605.
- [65] Klinowski J., Almeida Paz F. A., Silva P., Rocha J., (2011), Microwave-Assisted Synthesis of Metal-Organic Frameworks. *Dalton Transacti.* 40: 321-330.
- [66] Choi J.-Y., Kim J., Sung-Hwa J., Kim H.-K., Chang J.-S., Chae H. K., (2006), Microwave Synthesis of a Porous Metal-Organic Framework, Zinc Terephthalate MOF-5. *Bulleti. Korean Chem. Soc.* 27: 1523-1524.
- [67] Khan N. A., Jhung S. H., (2015), Synthesis of metal-organic frameworks (MOFs) with microwave or ultrasound: Rapid reaction, phase-selectivity, and size reduction. *Coordin. Chem. Rev.* 285: 11-23.
- [68] Furukawa H., Cordova K. E., O’Keeffe M., Yaghi O. M., (2013), The Chemistry and Applications of Metal-Organic Frameworks. *Science* 341.
- [69] Lickiss P. D., (2000), Ultrasound in Chemical Synthesis, *The New Chemistry.* pp. 76-84, Cambridge University Press.
- [70] Friščić T., Reid D. G., Halasz I., Stein R. S., Dinnebier R. E., Duer M. J., (2010), Ion- and Liquid-Assisted Grinding: Improved Mechanochemical Synthesis of Metal–Organic Frameworks Reveals Salt Inclusion and Anion Templating. *Angew. Chem. Int. Ed.* 49: 712-715.
- [71] Alavi M. A., Morsali A., (2014), Ultrasound assisted synthesis of {[Cu₂(BDC)₂(dabco)]₂DMF₂H₂O} nanostructures in the presence of modulator; new precursor to prepare nano copper oxides. *Ultrason. Sonochem.* 21: 674-680.
- [72] Li Z.-Q., Qiu L.-G., Xu T., Tu Y., Wang W., Wu Z.-Y., Jiang X., (2009), Ultrasonic synthesis of the microporous metal–organic framework Cu₃(BTC)₂ at ambient temperature and pressure: An efficient and environmentally friendly method. *Mater. Lett.* 63: 78-80.

- [73] Tahmasian A., Morsali A., (2012), Ultrasonic synthesis of a 3D Ni(II) Metal-organic framework at ambient temperature and pressure: New precursor for synthesis of nickel(II) oxide nano-particles. *Inorg. Chim. Acta.* 387: 327-331.
- [74] Fujishima A., Honda K., (1972), Electrochemical Photolysis of Water at a Semiconductor Electrode. *Nature.* 238: 37-38.
- [75] Khan M. M., Ansari S. A., Pradhan D., Ansari M. O., Han D. H., Lee J., Cho M. H., (2014), Band gap engineered TiO₂ nanoparticles for visible light induced photoelectrochemical and photocatalytic studies. *J. Mater. Chem. A.* 2: 637-644.
- [76] Nakata K., Fujishima A., (2012), TiO₂ photocatalysis: Design and applications. *Journal of Photochemistry and Photobiology C: Photochem. Rev.* 13: 169-189.
- [77] Zhang J., Zhou P., Liu J., Yu J., (2014), New understanding of the difference of photocatalytic activity among anatase, rutile and brookite TiO₂. *Physic. Chem. Chem. Phys.* 16: 20382-20386.
- [78] Gupta S. M., Tripathi M., (2011), A review of TiO₂ nanoparticles. *Chinese Sci. Bull.* 56: 1639-1657.
- [79] Beydoun D., Amal R., Low G., Mc Evoy S., (1999), Role of Nanoparticles in Photocatalysis. *J. Nanopart. Res.* 1: 439-458.
- [80] Kumar S. G., Rao K. S. R. K., (2015), Zinc oxide based photocatalysis: tailoring surface-bulk structure and related interfacial charge carrier dynamics for better environmental applications. *RSC Adv.* 5: 3306-3351.
- [81] Wang Q., Jiang H., Zang S., Li J., Wang Q., (2014), Gd, C, N and P quaternary doped anatase-TiO₂ nano-photocatalyst for enhanced photocatalytic degradation of 4-chlorophenol under simulated sunlight irradiation. *J. Alloys Comp.* 586: 411-419.
- [82] Rajbongshi B. M., Samdarshi S. K., (2014), Cobalt-doped zincblende-wurtzite mixed-phase ZnO photocatalyst nanoparticles with high activity in visible spectrum. *Appl. Catal. B: Environ.* 144: 435-441.
- [83] Mahata P., Madras G., Natarajan S., (2006), Novel Photocatalysts for the Decomposition of Organic Dyes Based on Metal-Organic Framework Compounds. *J. Phys. Chem. B.* 110: 13759-13768.
- [84] Tachikawa T., Choi J. R., Fujitsuka M., Majima T., (2008), Photoinduced Charge-Transfer Processes on MOF-5 Nanoparticles: Elucidating Differences between Metal-Organic Frameworks and Semiconductor Metal Oxides. *J. Phys. Chem. C.* 112: 14090-14101.
- [85] Llabrés i Xamena F. X., Corma A., Garcia H., (2007), Applications for Metal-Organic Frameworks (MOFs) as Quantum Dot Semiconductors. *J. Phys. Chem. C.* 111: 80-85.
- [86] Alvaro M., Carbonell E., Ferrer B., Llabrés i Xamena F. X., Garcia H., (2007), Semiconductor Behavior of a Metal-Organic Framework (MOF). *Chem. – A Europ. J.* 13: 5106-5112.
- [87] Hagfeldt A., Graetzel M., (1995), Light-Induced Redox Reactions in Nanocrystalline Systems. *Chem. Rev.* 95: 49-68.
- [88] Binnemans K., (2009), Lanthanide-Based Luminescent Hybrid Materials. *Chem. Rev.* 109: 4283-4374.
- [89] Allendorf M. D., Bauer C. A., Bhakta R. K., Houk R. J. T., (2009), Luminescent metal-organic frameworks. *Chem. Soc. Rev.* 38: 1330-1352.
- [90] Choi J. R., Tachikawa T., Fujitsuka M., Majima T., (2010), Europium-Based Metal-Organic Framework as a Photocatalyst for the One-Electron Oxidation of Organic Compounds. *Langmuir.* 26: 10437-10443.
- [91] Yang S. J., Im J. H., Kim T., Lee K., Park C. R., (2011), MOF-derived ZnO and ZnO@C composites with high photocatalytic activity and adsorption capacity. *J. Hazard. Mater.* 186: 376-382.
- [92] Kojima A., Teshima K., Shirai Y., Miyasaka T., (2009), Organometal Halide Perovskites as Visible-Light Sensitizers for Photovoltaic Cells. *J. Am. Chem. Soc.* 131: 6050-6051.
- [93] Walsh A., Catlow C. R. A., (2010), Photostimulated Reduction Processes in a Titania Hybrid Metal-Organic Framework. *Chem. Phys. Chem.* 11: 2341-2344.
- [94] Gascon J., Hernández-Alonso M. D., Almeida A. R., van Klink G. P. M., Kapteijn F., Mul G., (2008), Isorecticular MOFs as Efficient Photocatalysts with Tunable Band Gap: An Operando FTIR Study of the Photoinduced Oxidation of Propylene. *Chem. Sus. Chem.* 1: 981-983.
- [95] Du J.-J., Yuan Y.-P., Sun J.-X., Peng F.-M., Jiang X., Qiu L.-G., Xie A.-J., Shen Y.-H., Zhu J.-F., (2011), New photocatalysts based on MIL-53 metal-organic frameworks for the decolorization of methylene blue dye. *J. Hazard. Mater.* 190: 945-951.
- [96] Ai L., Zhang C., Li L., Jiang J., (2014), Iron terephthalate metal-organic framework: Revealing the effective activation of hydrogen peroxide for the degradation of organic dye under visible light irradiation. *Appl. Catal. B: Environ.* 148-149: 191-200.
- [97] Zhou T., Du Y., Borgna A., Hong J., Wang Y., Han J., Zhang W., Xu R., (2013), Post-synthesis modification of a metal-organic framework to construct a bifunctional photocatalyst for hydrogen production. *Energy & Environ. Sci.* 6: 3229-33.
- [98] Wang C., deKrafft K. E., Lin W., (2012), Pt nanoparticles@photoactive metal-organic frameworks: efficient hydrogen evolution via synergistic photoexcitation and electron injection. *J. Am. Chem. Soc.* 134: 7211-7214.
- [99] Wang X., Maeda K., Thomas A., Takanabe K., Xin G., Carlsson J. M., Domen K., Antonietti M., (2009), *Nat. Mater.* 8: 76-81.
- [100] Fateeva A., Chater P. A., Ireland C. P., Tahir A. A., Khimyak Y. Z., Wiper P. V., Darwent J. R., Rosseinsky M. J., (2012), A water-stable porphyrin-based metal-organic framework active for visible-light photocatalysis. *Angew. Chem. Int. Ed. Engl.* 51: 7440-7444.
- [101] Fu Y., Sun D., Chen Y., Huang R., Ding Z., Fu X., Li Z., (2012), An amine-functionalized titanium metal-organic framework photocatalyst with visible-light-induced activity for CO₂ reduction. *Angew. Chem. Int. Ed. Engl.* 51: 3364-3367.
- [102] Long J., Wang S., Ding Z., Wang S., Zhou Y., Huang L., Wang X., (2012), Amine-functionalized zirconium metal-organic framework as efficient visible-light photocatalyst for aerobic organic transformations. *Chem. Commun. (Camb)* 48: 11656-11658.
- [103] Horiuchi Y., Toyao T., Saito M., Mochizuki K., Iwata M., Higashimura H., Anpo M., Matsuoka M., (2012), Visible-Light-Promoted Photocatalytic Hydrogen Production by Using an Amino-Functionalized Ti(IV) Metal-Organic Framework. *J. Phys. Chem. C.* 116: 20848-20853.
- [104] Chatti R., Rayalu S. S., Dubey N., Labhsetwar N., Devotta S., (2007), Solar-based photoreduction of methyl orange using zeolite supported photocatalytic materials. *Solar Energy Mater. Solar Cells.* 91: 180-190.

- [105] Yu Y., Wang J., Parr J. F., (2012), Preparation and properties of TiO₂/fumed silica composite photocatalytic materials. *Procedia Eng.* 27: 448-456.
- [106] Artkla S., Wantala K., Srinameb B.-o., Grisdanurak N., Klysubun W., Wittayakun J., (2009), Characteristics and photocatalytic degradation of methyl orange on Ti-RH-MCM-41 and TiO₂/RH-MCM-41. *Korean J. Chem. Eng.* 26: 1556-1562.
- [107] Li Y., Li X., Li J., Yin J., (2006), Photocatalytic degradation of methyl orange by TiO₂-coated activated carbon and kinetic study. *Water Research* 40: 1119-1126.
- [108] Das M. C., Xu H., Wang Z., Srinivas G., Zhou W., Yue Y.-F., Nesterov V. N., Qian G., Chen B., (2011), A Zn4O-containing doubly interpenetrated porous metal-organic framework for photocatalytic decomposition of methyl orange. *Chem. Commun.* 47: 11715-11717.
- [109] Pu S., Xu L., Sun L., Du H., (2015), Tuning the optical properties of the zirconium–UiO-66 metal–organic framework for photocatalytic degradation of methyl orange. *Inorg. Chem. Commun.* 52: 50-52.
- [110] Zhu W., Yang X.-Y., Li Y.-H., Li J.-P., Wu D., Gao Y., Yi F.-Y., (2014), A novel porous molybdophosphate-based FeII,III-MOF showing selective dye degradation as a recyclable photocatalyst. *Inorg. Chem. Commun.* 49: 159-162.
- [111] Liang R., Jing F., Shen L., Qin N., Wu L., (2015), MIL-53(Fe) as a highly efficient bifunctional photocatalyst for the simultaneous reduction of Cr(VI) and oxidation of dyes. *J. Hazard. Mater.* 287: 364-372.
- [112] Liu C.-B., Sun H.-Y., Li X.-Y., Bai H.-Y., Cong Y., Ren A., Che G.-B., (2014), New photocatalyst for the degradation of organic dyes based on [Cu(ONCP)(4,42-BPDA)1/2(H₂O)·(4,42-H2BPDA)]n. *Inorg. Chem. Commun.* 47: 80-83.
- [113] Liu C.-B., Cong Y., Sun H.-Y., Che G.-B., (2014), Structure and photocatalytic performance of a new metal-organic framework based on [Zn(TBTC)(2,6-pydc)]n. *Inorg. Chem. Commun.* 47: 71-74.
- [114] Sun H.-Y., Liu C.-B., Cong Y., Yu M.-H., Bai H.-Y., Che G.-B., (2013), New photocatalyst for the degradation of organic dyes based on [Co₂(1,4-BDC)(NCP)₂]_n·4nH₂O. *Inorg. Chem. Commun.* 35: 130-134.

How to cite this article: (Vancouver style)

Majedi A., Davar F., Abbasi A. R., (2016), Metal-organic framework materials as nano photocatalyst. *Int. J. Nano Dimens.* 6 (5): 1-14.

DOI: [10.7508/ijnd.2016.01.001](https://doi.org/10.7508/ijnd.2016.01.001)

URL: http://ijnd.ir/article_15297_2444.html